

# Research And Application Of A Satellite Payload Heat Dissipation System

Zhibin Liu<sup>1,2</sup>, Weibing Dai<sup>1,2</sup>, Zaicheng Wang<sup>1,2</sup>, Qiang Zhang<sup>1,2</sup>, Chunsheng Yang<sup>1,2</sup>, Jinjun Yan<sup>1,2</sup>

<sup>1</sup>Beijing Institute of Spacecraft Environment Engineering, Beijing 100094, China

<sup>2</sup>Beijing Engineering Research Center of the Intelligent Assembly Technology and Equipment for Aerospace Product, Beijing 100094, china

E-mail: raindown@126.com

**Abstract.** Due to the installation of high power efficient payload heat dissipation instruments, the traditional fan cannot effectively reduce the working temperature of the instruments. It will cause the failure of the test. Therefore, based on the convection heat control method, the simulation and analysis of the model are carried out, and a payload heat dissipation system is built. The correctness of the model and calculation results is verified by experiments, which can effectively guarantee the smooth operation of instrument testing. This conclusion can provide a theoretical reference for other subsequent high-power payload heat dissipation devices.

## 1. Introduction

With the development of electronic technology, the volume of electronic products is becoming smaller and smaller, and the heat value is also increasing. High temperature can have a harmful effect on the performance of electronic devices, such as the high temperature will endanger the welding spot of the semiconductor, damage the connection interface of the circuit, increase the resistance of the conductor and form the mechanical stress damage [1]. Experiments and studies show that the system reliability will be reduced by 50% when the temperature of a single semiconductor element increases by 100°C, and the failure more than 55% of the electronic devices is due to the high temperature [2,3]. In order to ensure the normal and effective work of the instrument, a large amount of heat produced in the work must be taken away in time to ensure that the core and surface temperature of the instrument are maintained at a relatively low level. The lowering of the temperature of the instrument cannot only make its performance better, but also generate considerable economic efficiency [4].

The spacecraft thermal control technology is divided into two categories: passive thermal control and active thermal control. Passive thermal control includes temperature coating, heat pipe arrangement and so on. Active thermal control includes 3 forms: radiant heat control, convection heat control and conduction heat control.

At present, many domestic and foreign scholars have carried out theoretical and experimental studies on jet impingement heat transfer, such as Zu, Yan [5] and Zhang [6]. They analyze the flow and heat transfer characteristics of jet impingement under different turbulence models. Yang [7] analyses the heat dissipation performance of the semicircular concave surface under the jet impingement and gives the effect of the jet spacing on the heat dissipation performance of the system when the Reynolds number  $Re$  is fixed. In the ground test process, fans are often used as convection



heat control mode for heat dissipation. The heat load of a satellite payload instrument is very high. The traditional fan cannot effectively reduce the working temperature of the instrument, which leads to the failure of the test. Therefore, it is necessary to design the payload heat dissipation system to ensure the stability of the test work.

## 2. Modelling of the heat dissipation system of payload

### 2.1. Satellite parameters

40 high power payload instruments have been installed on one satellite. The thermal load of a single instrument is 68W. The size is long\*wide\*high =L\*H\*W=200.55 \*65 \*127.99 mm<sup>3</sup>. The exterior material is aluminium alloy, and the surface is coated with black heat control paint.

The size of the satellite communication module is simplified. The size of the module is as follows: length\*width\*height =X\*Y\*Z=2360\*2100\*2700mm<sup>3</sup>. The cabin is divided into two blocks, the north heat load is 2080W and the south heat load is 2260W. The north and south plates are made of aluminum plate by honeycomb core structure. The simplified view of the satellite communication module is shown in Figure 1.

The ambient temperature is 20 ± 5°C. The maximum temperature of the electronic device surface is 45 degrees.

The average temperature difference between the heat dissipation surface and the air temperature shows as Δt=20K; Δt=15K; Δt=10K.

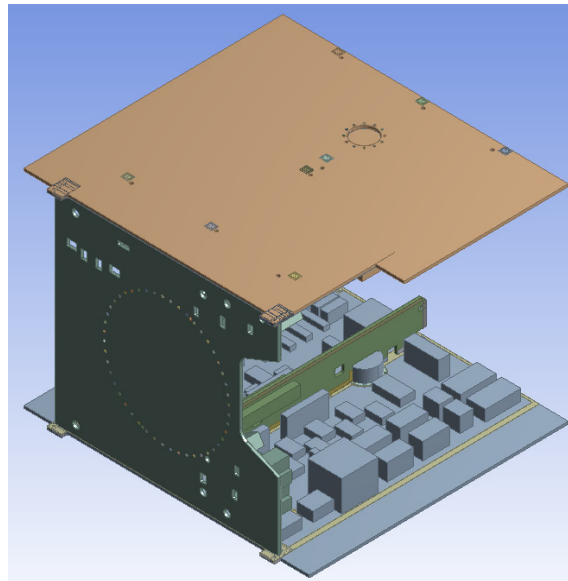


Figure 1. The simplified view of the satellite communication module.

### 2.2. Physical model

The calculation process includes two aspects: one is the numerical calculation of fluid flow and heat transfer coupling, the other one is the fluid solid coupling heat transfer calculation.

The three-dimensional steady heat conduction equation is as follows:

$$\nabla T = 0 \quad (1)$$

$$\frac{\partial^2 t}{\partial x^2} + \frac{\partial^2 t}{\partial y^2} + \frac{\partial^2 t}{\partial z^2} + \frac{\dot{\Phi}}{\lambda} = 0 \quad (2)$$

Air three-dimensional N-S equation:

$$\left\{ \begin{array}{l} \rho \left( \frac{\partial v_x}{\partial \tau} + v_x \frac{\partial v_x}{\partial x} + v_y \frac{\partial v_x}{\partial y} + v_z \frac{\partial v_x}{\partial z} \right) = \mu \left( \frac{\partial^2 v_x}{\partial x^2} + \frac{\partial^2 v_x}{\partial y^2} + \frac{\partial^2 v_x}{\partial z^2} \right) - \frac{\partial p}{\partial x} + \rho g_x \\ \rho \left( \frac{\partial v_y}{\partial \tau} + v_x \frac{\partial v_y}{\partial x} + v_y \frac{\partial v_y}{\partial y} + v_z \frac{\partial v_y}{\partial z} \right) = \mu \left( \frac{\partial^2 v_y}{\partial x^2} + \frac{\partial^2 v_y}{\partial y^2} + \frac{\partial^2 v_y}{\partial z^2} \right) - \frac{\partial p}{\partial y} + \rho g_y \\ \rho \left( \frac{\partial v_z}{\partial \tau} + v_x \frac{\partial v_z}{\partial x} + v_y \frac{\partial v_z}{\partial y} + v_z \frac{\partial v_z}{\partial z} \right) = \mu \left( \frac{\partial^2 v_z}{\partial x^2} + \frac{\partial^2 v_z}{\partial y^2} + \frac{\partial^2 v_z}{\partial z^2} \right) - \frac{\partial p}{\partial z} + \rho g_z \end{array} \right. \quad (3)$$

### 2.3. Model gridding

We take the 1/4 area as the research object. Figure 2 is the grid diagram of the south plate view model. Icepak software is used to analyse the heat dissipation of each module. The specific Settings are as follows:

Ambient pressure: an atmospheric pressure;

Ambient temperature: 20 degrees centigrade;

Fluid type: Turbulent;

Grid type: Mesher-HD;

Max X size = 0.16, Max Y size = 0.09, Max Z size = 0.14, Minimum gap: 0.001m;

Iteration steps: 500;

Convergence factor : pressure 0.3;

Momentum: 0.7;

The convergent value of the residual curve: Flow: 0.001;

Energy:  $1e^{-7}$ ;

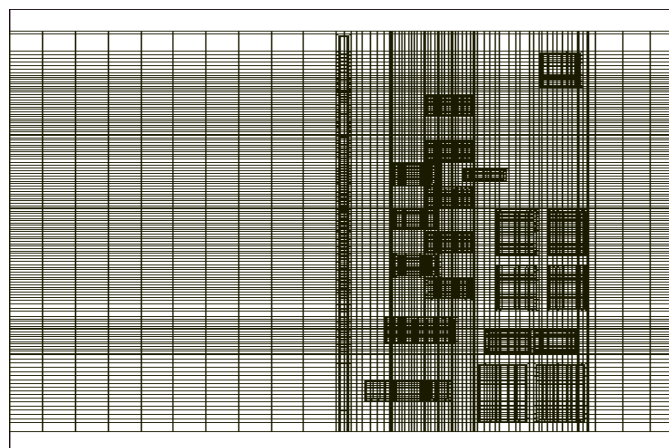


Figure 2. The grid diagram of the south plate view model.

### 3. Calculation results and analysis

The maximum temperature of the instrument is  $80^{\circ}\text{C}$ . The target heat dissipation temperature should be reduced to below  $50^{\circ}\text{C}$ . The numerical simulation of the flow field, temperature field and pressure distribution are carried out. The results are described in Table 1.

Table 1. Summary of calculation results.

Working condition	Total air volume	Ambient temperature	Ambient pressure	Maximum surface temperature of instrument	Main stream speed	Maximum absolute pressure
1	0.95 m <sup>3</sup> /s	20°C	101325 Pa	42.39°C	11.2 m/s	812.5 Pa
2	1.15 m <sup>3</sup> /s	20°C	101325 Pa	36.60°C	18.13 m/s	820.65 Pa
3	1.15 m <sup>3</sup> /s	25°C	101325 Pa	41.61°C	13.1 m/s	820.65 Pa

The results of simulation analysis are presented in the case of the following conditions: total air volume: 1.15 m<sup>3</sup>/s, ambient temperature: T=25 C, ambient pressure: 101325Pa. The temperature distribution of the instrument is shown in Figure 3. The velocity field in the vertical section is shown in Figure 4. The velocity of the main surface of the instrument is shown as the black point in the figure 5. The distribution of the pressure field in the Y direction is shown in Figure 6.

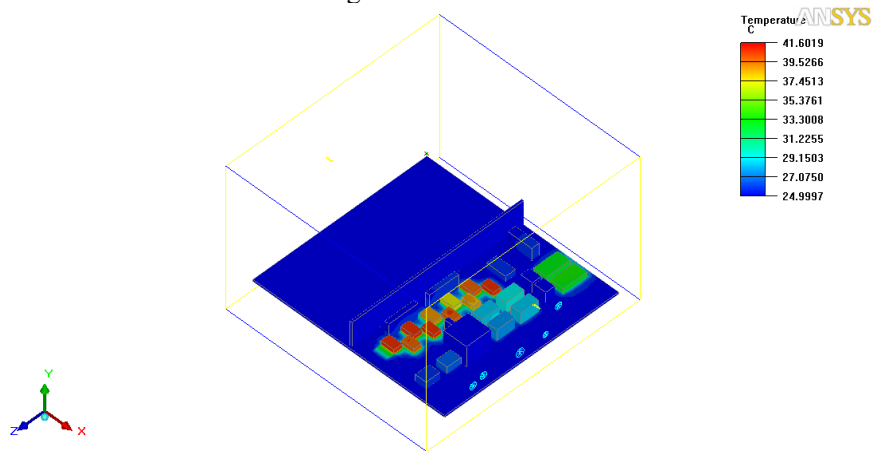


Figure 3. Schematic diagram of the temperature distribution of the instrument.

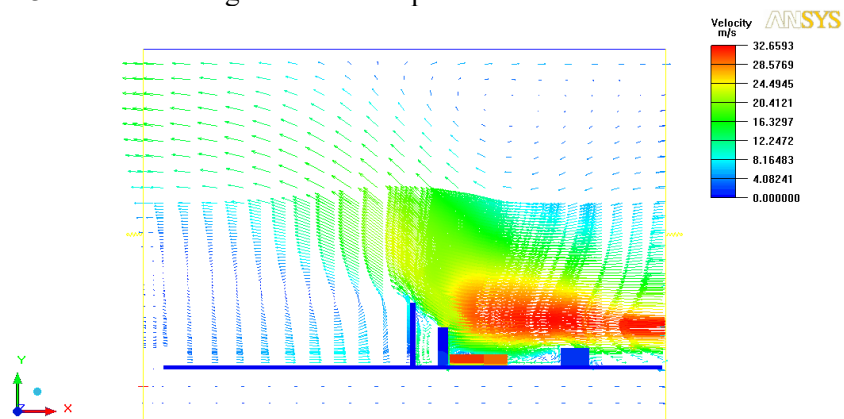


Figure 4. Schematic diagram of velocity field distribution in vertical direction.

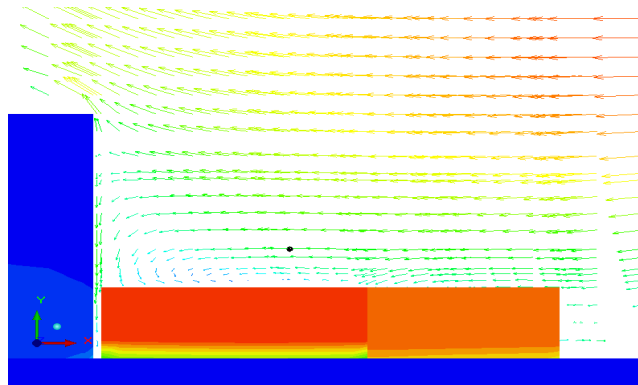


Figure 5. Schematic diagram of the main area of the instrument surface.

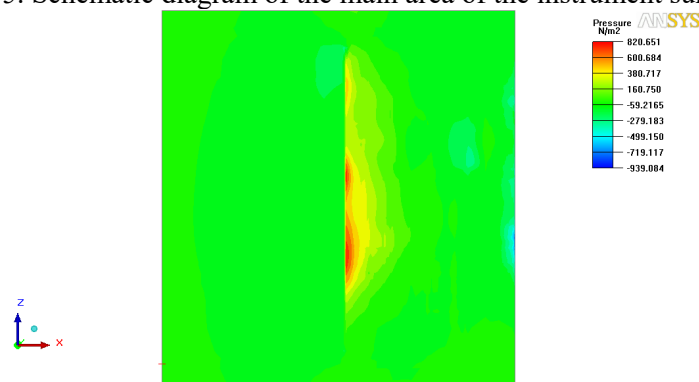


Figure 6. Schematic diagram of the distribution of pressure field in the Y direction.

After calculation, we can see that the convection thermal control method can meet the needs of instrument testing.

#### 4. The composition of the heat dissipation system of the payload

The payload heat dissipation system consists of two parts, including payload heat dissipation equipment and payload heat dissipation tooling.

##### 4.1. Payload heat dissipation equipment

Payload heat dissipation equipment includes the following 4 parts. The schematic diagram of the communication module is shown in Figure 7.

Ambient pressure: an atmospheric pressure;

- 1) the air-cooled mainframe.
- 2) main air duct: amount 4, length 10m, diameter 250mm, it can connect air-cooled mainframe and confluence.
- 3) junction station: amount 4, each can divide one airflow into 10 parts.
- 4) fine air duct: amount a lot, the length is 0.5m to 5m, diameter 50mm, it can connect the junction station for sending the wind to the surface of the instrument, or the corresponding position of the instrument outside the cabin.

##### 4.2. Payload heat dissipation tooling

The payload heat dissipation tooling includes the following 4 parts. Figure 8 shows the whole star working condition diagram:

- 1) mobile car: providing two levels of mobility.
- 2) vertical beam: supporting the main air duct and the junction station.
- 3) cantilever beam: supporting fine air duct.
- 4) output interface: aligning the target of heat dissipation.

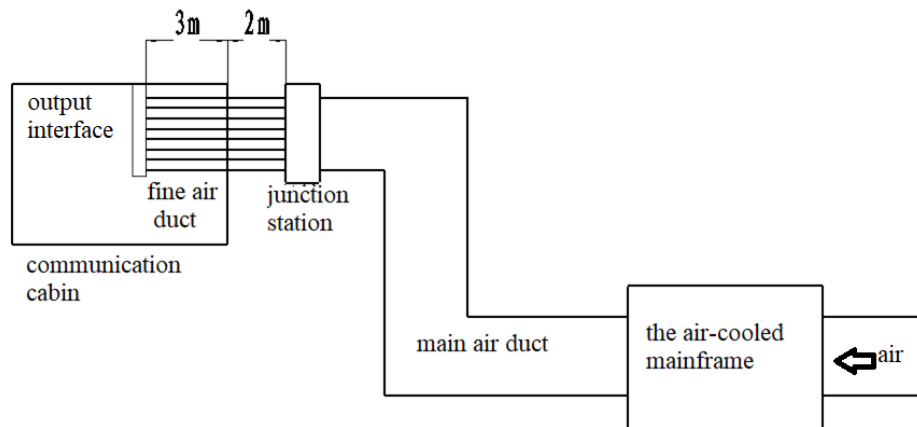


Figure 7. Schematic diagram of the working condition of the communication cabin.

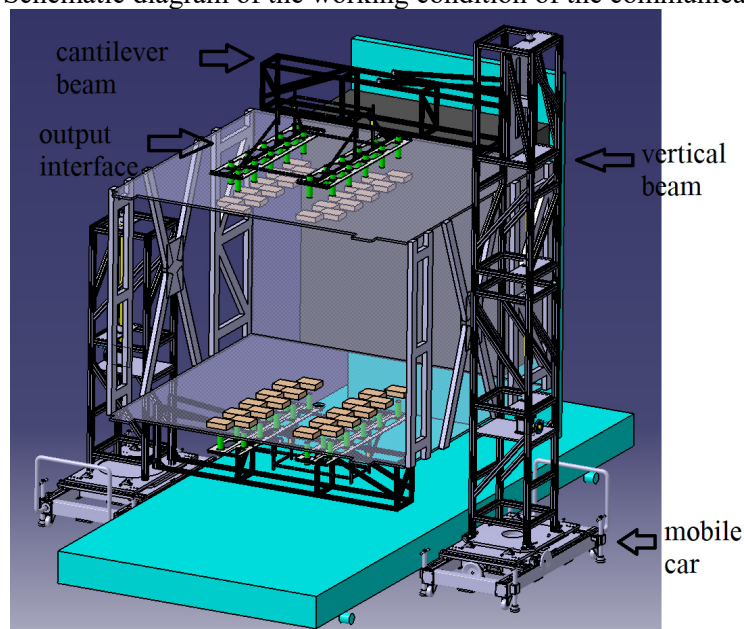


Figure 8. Schematic diagram of the working condition of the whole star.

Payload heat dissipation tooling finish the test under the actual working condition. Under the condition that the wind speed of the end form the fine air duct is 13.1m/s, the surface temperature of the instrument is kept below 50 C during the whole test.

## 5. Conclusion

This paper sets up a model based on the convection heat control method and the heat dissipation characteristics of air jet. Modelling, grid analysis and calculation are carried out. According to the calculation structure, a payload heat dissipation system is set up. In the test process, it can be seen that the surface temperature of the instrument is always below 50 degrees centigrade under the condition of 13.1m/s. The test task can be completed satisfactorily. There will be no test stop due to the high temperature of the instrument. The safety is greatly reduced. A payload heat dissipation system can greatly reduce the probability of occurrence of security problems, effectively protect the quality and progress of satellite assembly development.

## References

- [1] Viswannath R, Nair R and Wakharkar Emerging directions for packaging technologies 2002 *J. Intel Technology Journal.* 6 61-74

- [2] Performance characteristics of IC packages. Inter technical documents.  
<http://developer.intel.com>
- [3] Teng Li and Jing Liu Latest research advancement and assessment of chip cooling techniques 2004 *J. Journal of refrigeration*. **3** 22-32
- [4] Changgeng Li Research on cooling method of electronic devices based on impinging jet 2009 *D. Central South University. Doctoral dissertations* p 63
- [5] Yang Y T, Wei T C and Wang Y H Numerical study of turbulent slot jet impingement cooling on a semi-circular concave surface 2010 *J. International Journal of Heat and Mass Transfer* **54** 482-489
- [6] Huang C H, Chen Y H and Li H Y An impingement heat sink module design problem in determining optimal nonuniform fin widths 2013 *J. International Journal of Heat and Mass Transfer* **67** 992-1006
- [7] Huang C H and Chen Y H An impingement heat sink module design problem in determining simultaneously the optimal nonuniform fin widths and heights 2014 *J. International Journal of Heat and Mass Transfer* **73** 627-633